

Supplementary Information

Reference Material of Prussian Blue Nanozymes for the Peroxidase-like Activity

Haijiao Dong ^a, Guancheng Wang ^a, Kaizheng Feng ^a, Xiaohan Wu ^a, Yaoyao Fan ^a, Wei Zhang ^b,

Ming Ma ^{a,*}, Ning Gu ^{a,*} and Yu Zhang ^{a,*}

^a *State Key Laboratory of Bioelectronics, Jiangsu Key Laboratory for Biomaterials and Devices, School of Biological Science and Medical Engineering & Collaborative Innovation Center of Suzhou Nano Science and Technology, Southeast University, Nanjing 210096, P. R. China*

^b *Department of General Surgery, the First Affiliated Hospital of Nanjing Medical University, Nanjing 210029, P.R. China*

** Corresponding author:*

Yu Zhang, Ph.D.

Professor

Ming Ma, Ph.D

Associate professor

Ning Gu, Ph.D

Professor

State Key Laboratory of Bioelectronics, Jiangsu Key Laboratory for Biomaterials and Devices,

School of Biological Science and Medical Engineering, Southeast University

87 Dingjiaqiao, District Gulou, Nanjing 210009, China

Tel: (86) 25-8327 2496.

E-mail: zhangyu@seu.edu.cn; maming@seu.edu.cn; guning@seu.edu.cn

Content

- 1. Supplementary Figures:** Fig. S1-S7
- 2. Supplementary Tables:** Table S1-S5
- 3. Supplementary Texts:** Section A-D
- 4. References**

Supplementary Figures

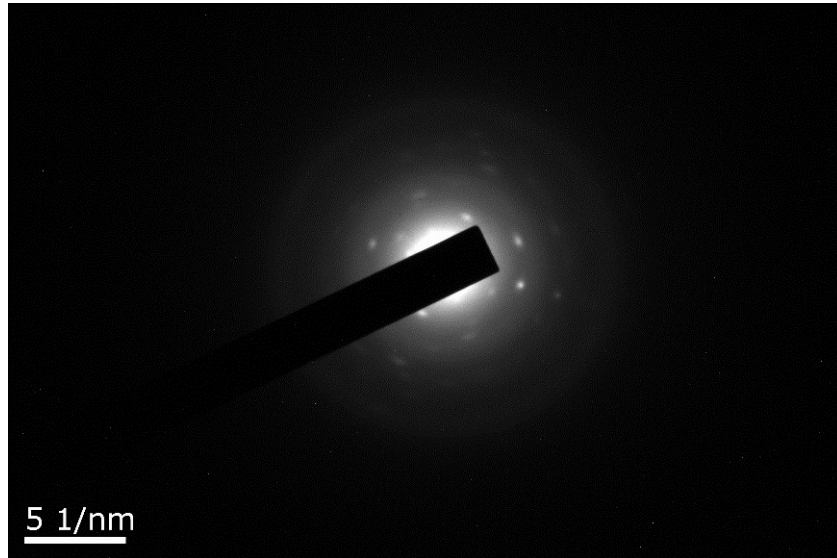


Fig. S1 The selective area electron diffraction (SAED) image of PBNEs.

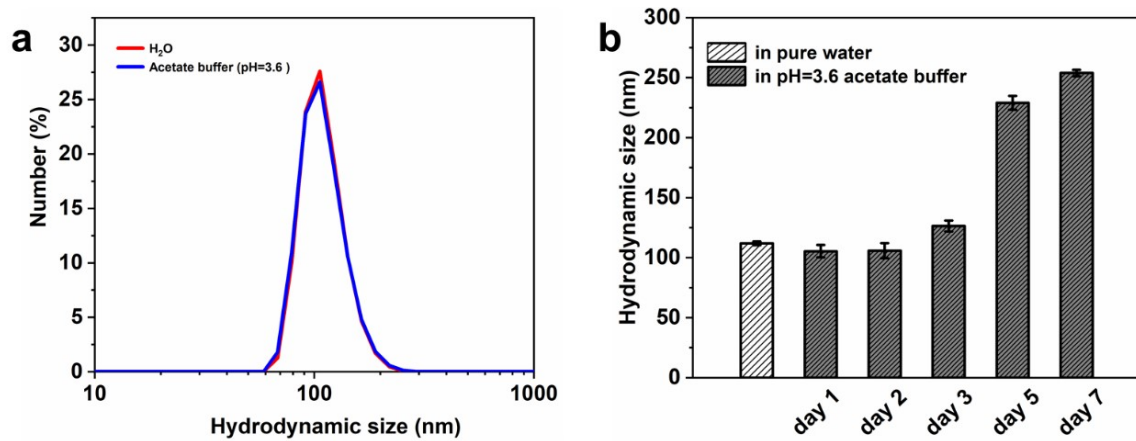


Fig. S2 (a) The hydrodynamic diameter of PBNEs dissolved in H₂O and acetate buffer. (b) Variation of the hydrodynamic diameter of PBNEs dissolved in acetate buffer solution (pH=3.6) during a week.

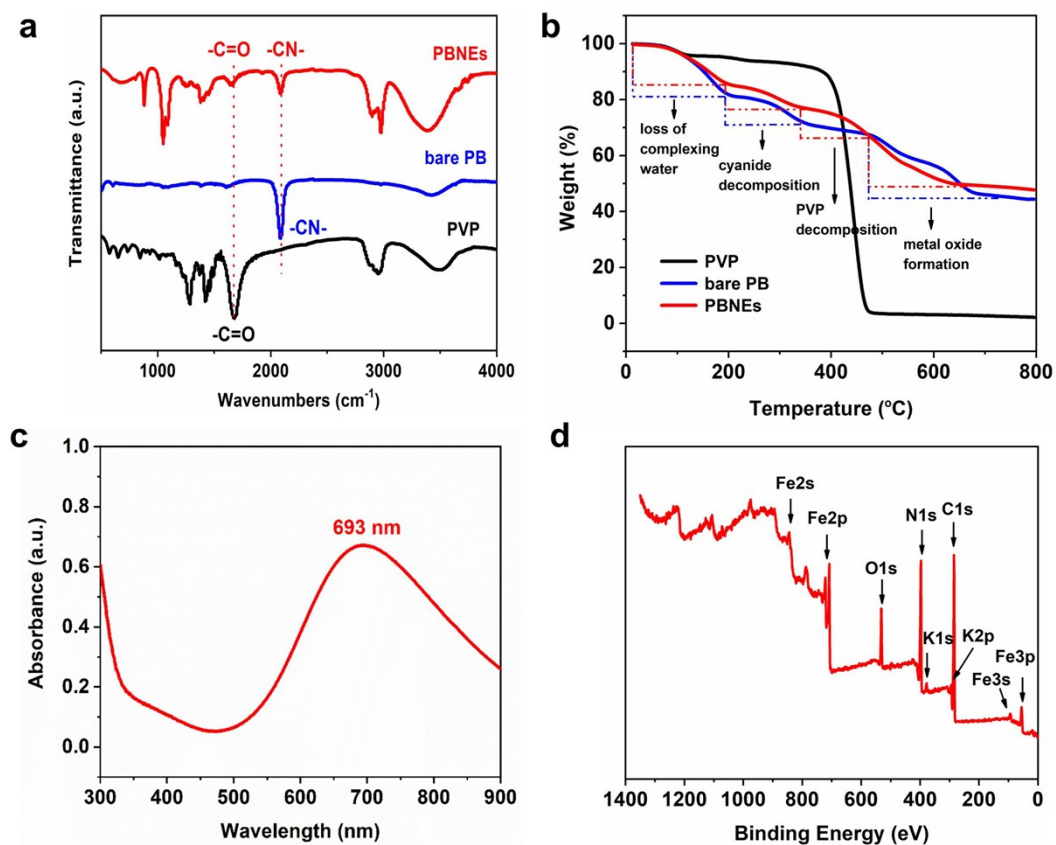


Fig. S3 (a) FTIR spectrum and (b) TG curves of PVP, bare PB and PBNEs. (c) UV-Vis absorption spectrum of PBNEs. (d) Survey XPS spectrum of PBNEs.

Fig. S3b: The weightlessness of bare PB was divided into three stages: the loss of complexing water from room temperature to 192 $^{\circ}\text{C}$; cyanide decomposed into nitrate between 234 $^{\circ}\text{C}$ and 344 $^{\circ}\text{C}$; and nitrate completely decomposed into metal oxide from 475 $^{\circ}\text{C}$ to 683 $^{\circ}\text{C}$. Compared to bare PB, an additional stage of PVP decomposition could be observed in PBNEs from 360 $^{\circ}\text{C}$ to 500 $^{\circ}\text{C}$, proving the successful modification of PVP on the surface of PB. It was calculated that PVP accounted for 11% of the total mass of PBNEs.

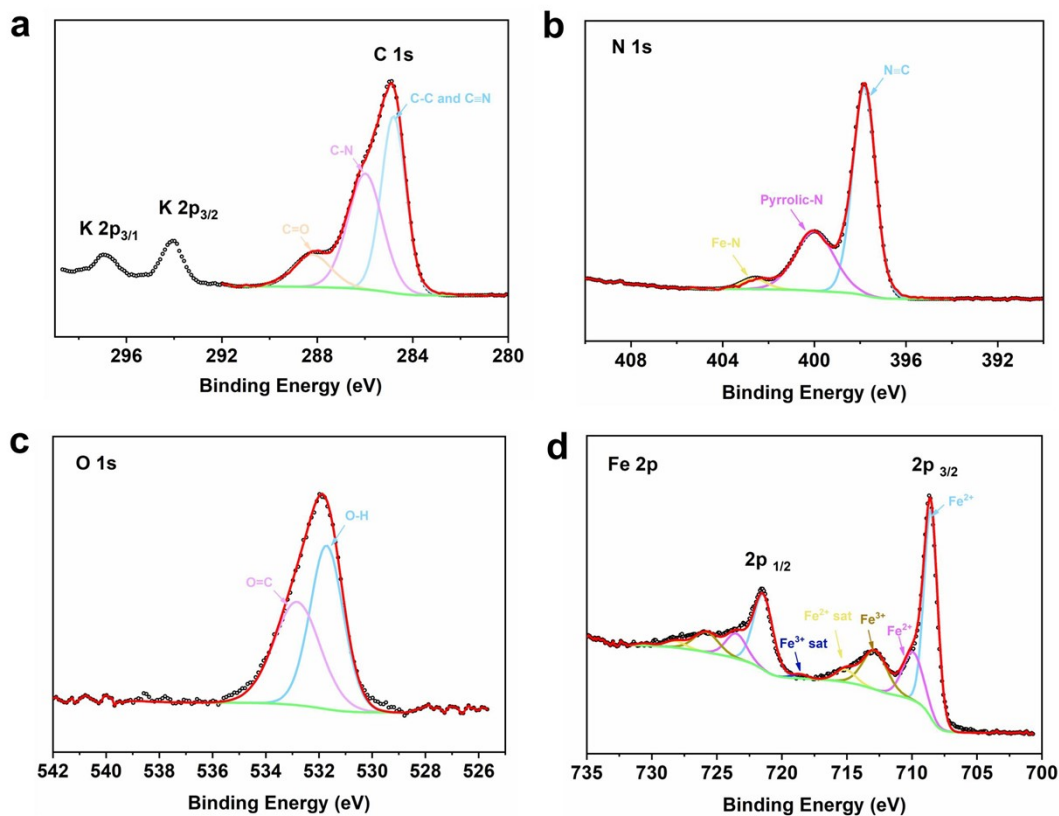


Fig. S4 The fitting XPS spectra of PBNEs. (a) C 1s and K 2p; (b) N 1s; (c) O 1s; (d) Fe 2p.

The fitted C1s and N1s peak indicated the existence of $C \equiv N$, $C=O$ and pyrrolic-N, agreeing well with the results of FTIR. The Fe 2p_{3/2} peak could be deconvoluted into five peaks, which were assigned to Fe²⁺ at 708.5 eV and 709.9 eV, Fe³⁺ at 712.8 eV, Fe²⁺ satellite peak at 715.1 eV, and Fe³⁺ satellite peak at 718.6 eV, respectively.¹

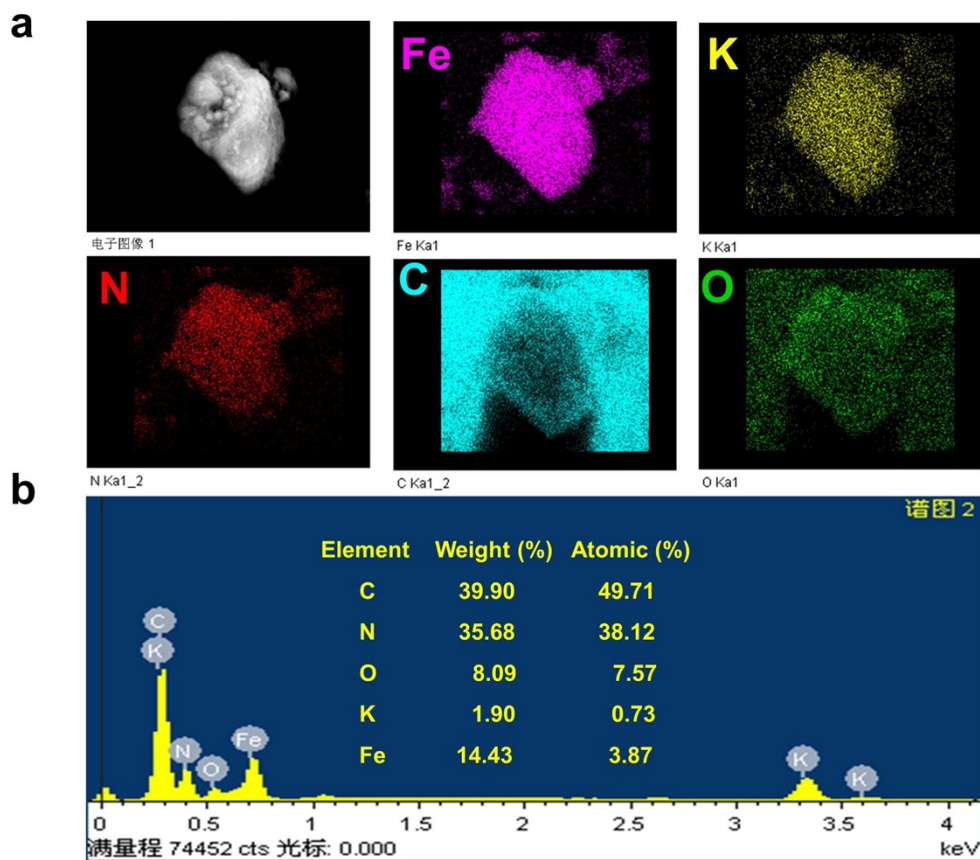


Fig. S5 X-ray mapping images and EDS spectra of PBNEs.

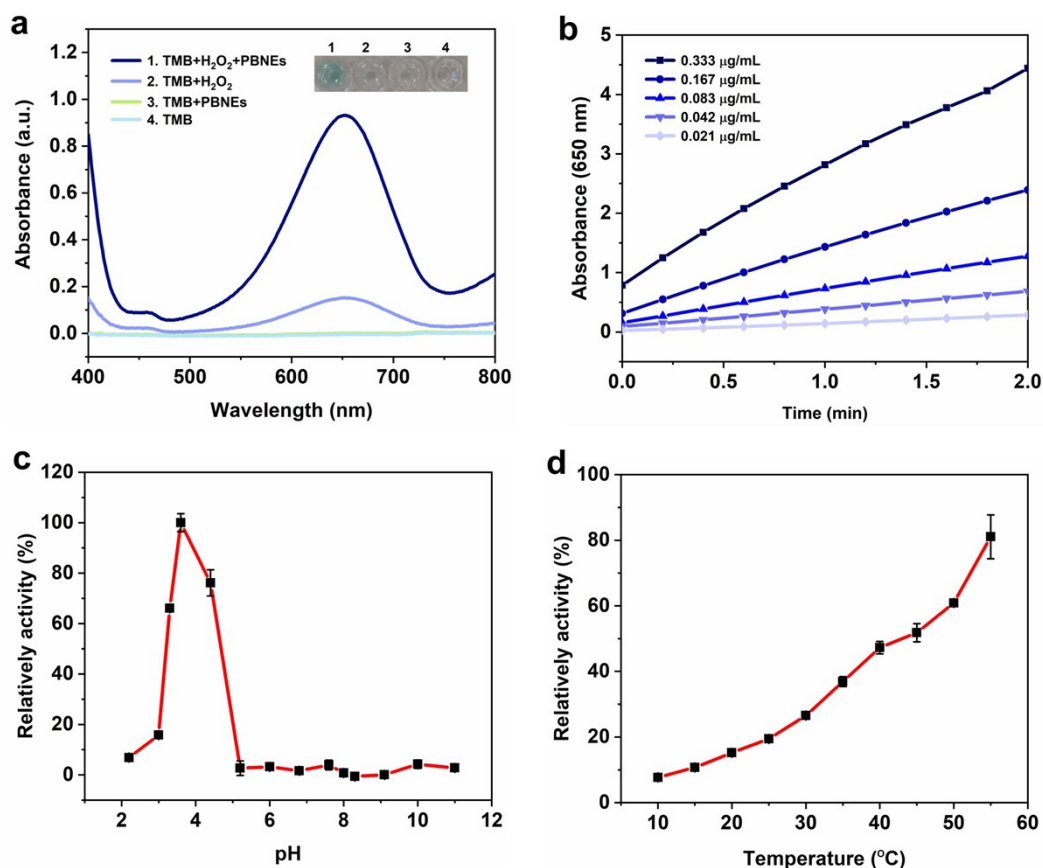


Fig. S6 (a) UV-visible absorption spectra of 1. TMB + H₂O₂ + PBNEs, 2. TMB + H₂O₂, 3. TMB + PBNEs, and 4. TMB. Inset: Corresponding digital photograph of the reaction systems. Experiments were carried out using 0.042 μg Fe·mL⁻¹ PBNEs, and/or 0.83 M H₂O₂ in 0.2 M acetate buffer (pH = 3.6), with 1.73 mM TMB as substrate. (b) Time-dependent absorption changes at 650 nm in the presence of different concentrations of PBNEs. (c) pH and (d) temperature dependent POD-like activity of PBNEs. Error bars represent at least three independent measurements.

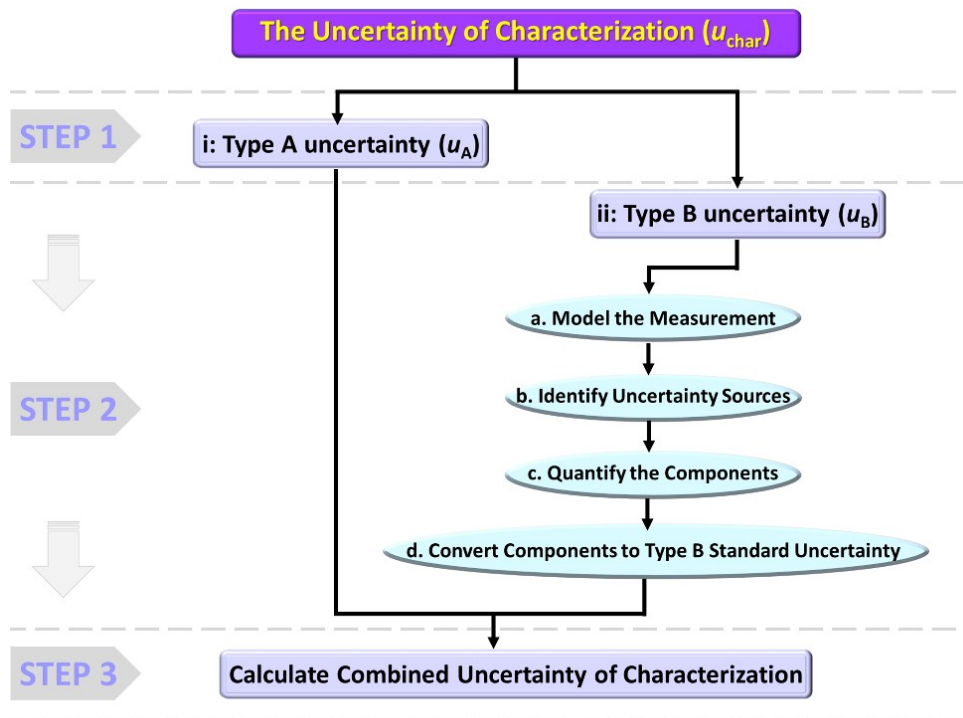


Fig. S7 The uncertainty evaluation process of characterization.

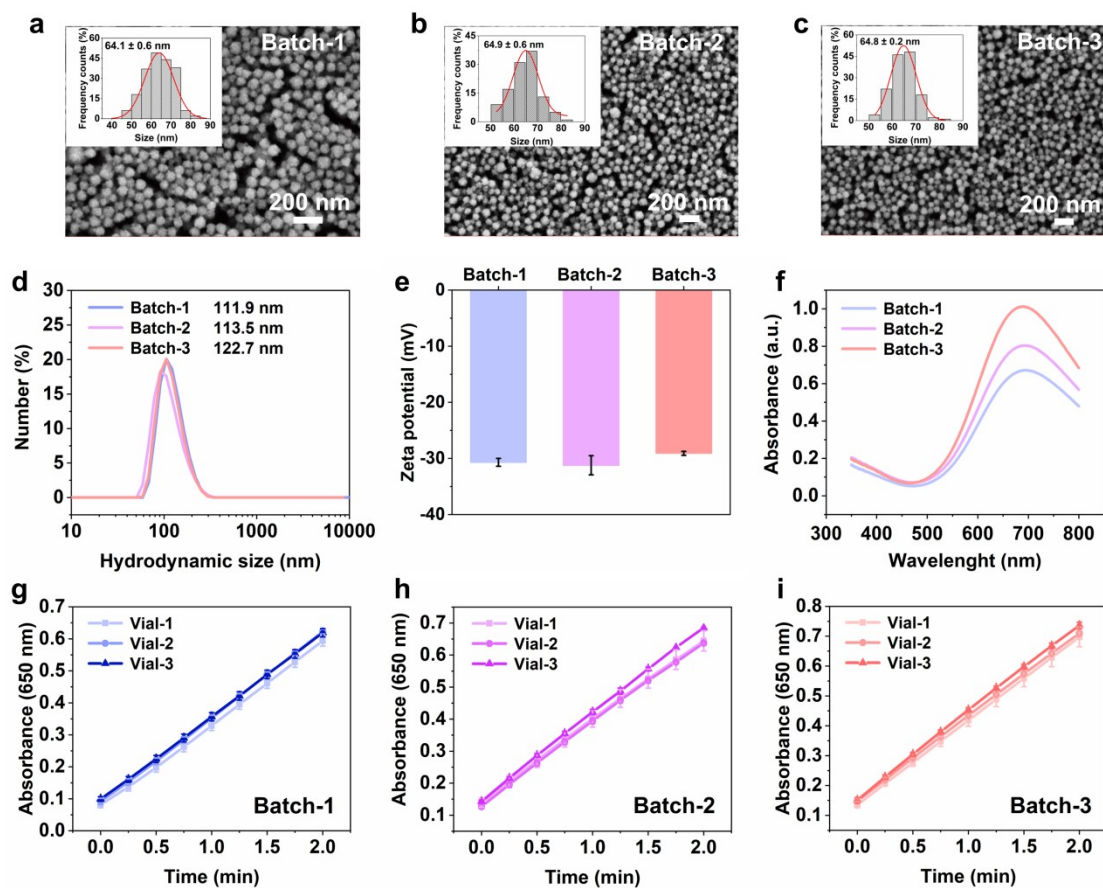


Fig. S8 Inter-batch consistency study of PBNEs CRM. (a-c) SEM images and size distribution histograms, (d) hydrodynamic diameter, (e) surface potential, (f) UV absorbance spectra, and (g-i) the POD-like activity measurement of three batches of PBNEs.

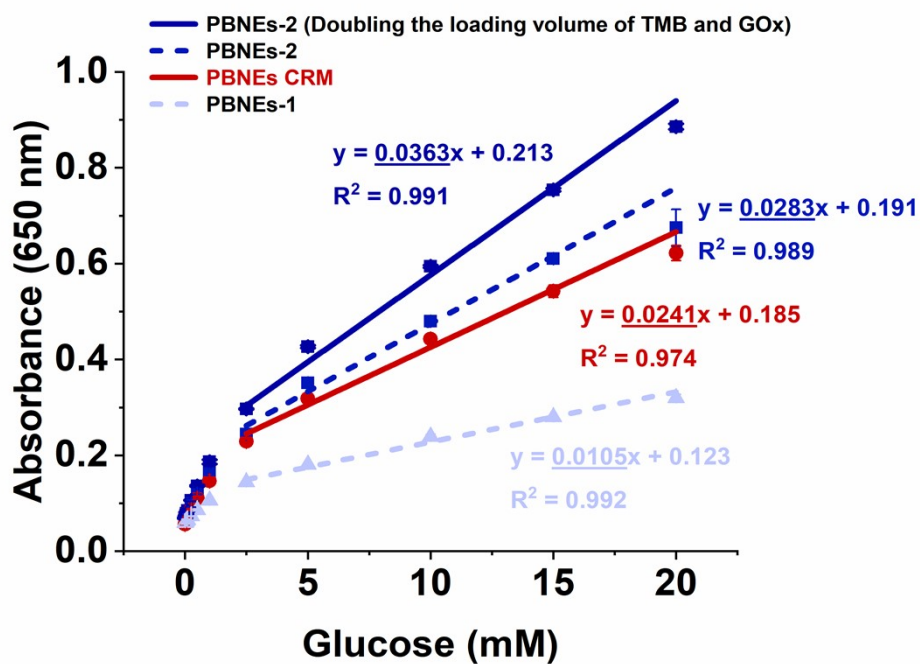


Fig. S9 Calibration curves of Glu for wet chemistry method. The activity concentrations of PBNEs directly affects the analytical results.

Table S1 Measurement data (a_{nano}) of homogeneity assessment for the POD-like activity of PBNEs CRM.

Note: 15 vials of PBNEs were randomly selected from 100 sample units. Each vial was measured independently 3

Vial		a_{nano} (U • mg ⁻¹)				Vial		a_{nano} (U • mg ⁻¹)			
NO.	n=1	n=2	n=3	Mean (\bar{x}_i)	No.	n=1	n=2	n=3	Mean (\bar{x}_i)		
1	168.31	158.87	162.12	163.10	9	159.65	154.56	162.57	158.93		
2	172.94	160.06	158.44	163.81	10	173.25	175.14	175.79	174.73		
3	171.89	163.82	156.91	164.21	11	162.76	163.40	163.84	163.34		
4	164.179	159.20	170.43	164.60	12	173.92	166.09	157.67	165.90		
5	166.599	172.22	173.28	170.70	13	167.33	172.42	163.31	167.69		
6	165.58	159.67	159.46	161.57	14	160.49	158.38	173.57	164.15		
7	176.03	166.19	163.50	168.57	15	166.87	159.99	168.58	165.15		
8	171.94	169.73	168.81	170.16	Arithmetic mean of \bar{x}_i ($\bar{\bar{x}}$)				165.77		

times under the repeatable conditions.

Table S2 Measurement results of long-term stability for the POD-like activity of PBNEs CRM.

Time (month)	a_{nano} (U • mg ⁻¹)
0	162.50
0.5	170.22
1	162.65
2	165.97
4	163.74
6	173.13
9	163.92
12	161.84
Arithmetic mean	165.50
Standard deviation	4.09
Relative standard deviation	2.47 %

Table S3 Interlaboratory comparison results of characterization with 8 laboratories.

NO.	Characterization laboratory	\bar{a}_{inano} (U·mg ⁻¹)
1	Jiangsu Key Laboratory for Biomaterials and Devices, Southeast University	164.65
2	State Key Laboratory of Bioelectronics, Southeast University	182.13
3	State Key Laboratory of Coordination Chemistry, Nanjing University	173.33
4	National Laboratory of Solid State Microstructures, Nanjing University	167.54
5	College of Sciences, Nanjing Agricultural University	181.70
6	Second Affiliated Hospital of Nanjing Medical University	180.74
7	School of Environmental and Biological Engineering, Nanjing University of Science and Technology	169.07
8	College of Science, Nanjing University of Aeronautics and Astronautics	171.88
	Arithmetic Mean (\bar{a}_{nano})	174

Table S4 Uncertainty of the relevant reagents and apparatuses.

Reagents and Apparatus	Value	Standard uncertainty	Relative standard uncertainty
------------------------	-------	----------------------	-------------------------------

		$U_c(x)$	$U_c(x)/x$
Fe element standard solution	1000 $\mu\text{g/mL}$	4.04151 $\mu\text{g/mL}$	4.04151×10^{-3}
Pipettor	200 μL	0.06 μL	3×10^{-4}
Pipettor	1000 μL	0.27 μL	2.7×10^{-4}
Volumetric flask	50 mL	0.0075 mL	1.5×10^{-4}
Volumetric flask	500 mL	0.035 mL	7×10^{-5}
The optical path of cuvette	1.004 cm	0.00006 cm	6.0×10^{-5}
UV-Vis spectrophotometer	-	0.003	-

Table S5 Inter-batch consistency study of PBNEs CRM.

Batch NO.	Particle size	Hydrodynamic diameter	Zeta potential	Maximum UV absorption peak	The POD-like activity
-----------	---------------	-----------------------	----------------	----------------------------	-----------------------

	(nm)	(nm)	(mV)	(nm)	(a_{nano} , U·mg ⁻¹)
1	64.1	111.9	-30.7	696.5	164.65
2	64.9	113.5	-31.2	696.0	168.79
3	64.8	122.7	-29.1	694.0	175.81
Arithmetic mean	64.6	116.0	-30.3	695.5	169.75
Standard deviation (SD)	0.44	5.848	1.11	1.323	5.642
Coefficient of variation (CV)	0.67%	2.47%	3.66%	0.19 %	3.32%

Table S6 Detection results of glucose in real samples.

Sample	Proposed method (mM)	Commercial kit (mM)	Relative deviation (%)
Glucose injection	246 ± 4.88	241 ± 9.01	1.66
Coca-cola	252 ± 4.08	235 ± 4.68	7.59
Milky tea	15.6 ± 1.17	15.5 ± 0.73	0.46
Lactobacillus drink	16.6 ± 0.49	17.8 ± 0.58	-7.15

Supplementary Texts

Section A

Reagents and sample preparation

A.1 Reagents preparation²

A.1.1 0.2 M Acetate buffer solution (pH = 3.6)

Add 8 mL of pure water containing 0.164 g of sodium acetate to 10 mL volumetric flask. 0.2 M of sodium acetate solution is prepared by adding pure water to the scale mark.

Add 80 mL of pure water containing 1.144 mL of glacial acetic acid to 100 mL volumetric flask. 0.2 M of glacial acetic acid solution is prepared by adding pure water to the scale mark.

Mix above two solutions in a certain proportion to prepare 0.2 M acetate buffer solution with a pH of 3.6 (25 °C).

A.1.2 10 mg·mL⁻¹ TMB

Add 8 mL of DMSO containing 0.10 g of TMB to 10 mL volumetric flask. 10 mg/mL of TMB is prepared by adding DMSO to the scale mark. The shelf life is 1 month at 2~8 °C in dark. It is recommended to store in separate packages. It shall be fully dissolved when used and avoid repeated freezing-thawing. The solution is strictly prohibited to use if the colour or absorption spectrum changed.

A.2 Sample preparation and subpackage

A.2.1 The measurement of Fe element mass concentration of PBNEs

A.2.1.1 The establishment of working curve

The working curve of Fe element standard solution was established by 1,10-phenanthroline spectrophotometry. First, 20, 40, 60, 80, and 100 µL of Fe element standard solution ($C_s = 1000 \mu\text{g}\cdot\text{mL}^{-1}$) were acidified with 2 mL of 6 M HCl and reduced with 1 mL of 10% hydroxylamine hydrochloride, respectively. After color

reaction with 2 mL of 0.1% 1,10 phenanthroline, the pH of the solution was adjusted to about 5 with 2 mL of 6 M NaOH and 5 mL of acetate buffer solution (pH=5) and the volume was fixed to 50 mL with pure water. The absorbance of these solutions at 510 nm was measured with UV-vis spectrophotometer (Table A.1).

Table A.1 Absorbance measurement of Fe element standard solutions with different mass concentrations

The mass concentration of Fe element (C , unit: $\mu\text{g}/50 \text{ mL}$)	Absorbance at 510 nm (A)			
	n=1	n=2	n=3	Mean
20	0.090	0.093	0.089	0.0907
40	0.176	0.17	0.169	0.1717
60	0.250	0.251	0.251	0.2507
80	0.332	0.329	0.328	0.3297
100	0.412	0.407	0.415	0.4113

Note : Three measurements were repeated for each concentration group (n=3).

The working curve of absorbance changing with Fe element mass concentrations was obtained by liner fitting the data from Table A.1 (Fig A.1). The C-A linear equation was shown in Eq. A.1.

$$A = 0.004C + 0.011 \dots \dots \dots (A.1)$$

where A is the absorbance of solution at 510 nm; C is the mass concentration of Fe element in a constant volume of 50 mL ($\mu\text{g} \cdot 50 \text{ mL}^{-1}$).

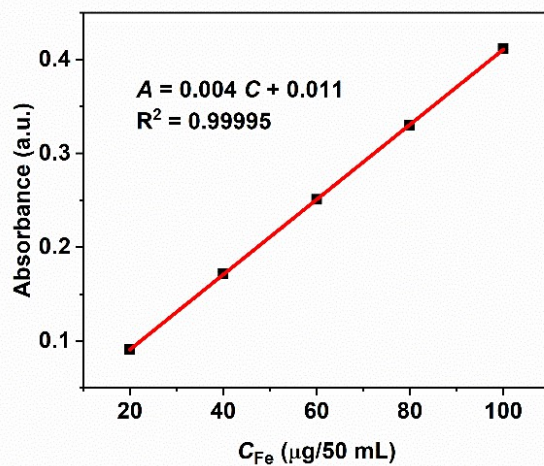


Fig A.1 The working curve of absorbance changing with Fe element mass concentrations

A.2.1.2 Fe element mass concentration of PBNEs

50 μL of the as-synthesized PBNEs was transferred into a crucible and calcined at 350 $^{\circ}\text{C}$ in muffle furnace for 5 h in order to completely oxidize to iron oxide. 2.5 mL of 6 M HCl was used to fully dissolve the iron oxide to obtain the iron ion solution. Transferring 2 mL of iron ion solution (corresponding to 40 μL of the as-synthesized PBNEs) into a 50 mL volumetric flask and the Fe element mass concentration was measured according to the method specified in A.2.1.1. Three groups of parallel control were conducted and each group was measured for five times. The mean value of the absorbance at 510 nm was used to calculate the Fe element mass concentration of 40 μL of as-synthesized PBNEs according to Eq. A.1. The measurement and calculation results were shown in Table A.2.

Table A.2 Data statistics of the measurement of Fe element mass concentration for the as-synthesized PBNEs

Group	Absorbance at 510 nm (A)					Mean		C_m ($\mu\text{g}\cdot 50\text{ mL}^{-1}$)
	1	2	3	4	5	\bar{A}	$\bar{\bar{A}}$	
	1	0.147	0.152	0.154	0.152	0.148	0.1506	
2	0.145	0.144	0.149	0.156	0.152	0.1492	0.155	36.05
3	0.161	0.162	0.169	0.169	0.168	0.1658	2	

The Fe element mass concentration of the as-synthesized PBNEs (C_0):

$$C_0 = 36.05 \mu\text{g} \div 40 \mu\text{L} = 0.90125 \mu\text{g} / \mu\text{L}$$

A.2.2 Sample subpackage

554.8 μL of the as-synthesized PBNEs ($0.90125 \mu\text{g} \cdot \mu\text{L}^{-1}$) was transferred into a 500 mL volumetric flask. Adding pure water to the scale mark ($20 \text{ }^\circ\text{C}$) to obtain $1 \mu\text{g} \cdot \text{mL}^{-1}$ PBNEs solution, which was dispensed into brown glass vial with 5 mL per each (the minimum packing unit, Fig A.2). A batch of PBNEs CRM candidates including 100 units was produced and stored at $4 \text{ }^\circ\text{C}$ for subsequent experiments.



Fig A.2 Digital photograph of PBNEs CRM candidates (5 mL/vial, total 100 vials).

Section B

Long-term stability assessment of POD-like activity for PBNEs CRM

by regression analysis

The linear regression analysis of POD-like activity (Y_i) with storage time (X_i) was carried out by substituting the data in Table 2 into Eq. B.1.

$$Y_i = \beta_0 + \beta_1 X_i \dots \dots \dots (B.1)$$

where β_1 is the slope of the regression function, and can be calculated by

$$\beta_1 = \frac{\sum_{i=1}^n (X_i - \bar{X})(Y_i - \bar{Y})}{\sum_{i=1}^n (X_i - \bar{X})^2} = -0.14$$

; β_0 is the intercept of the regression function, and

can be calculated by $\beta_0 = \bar{Y} - \beta_1 \bar{X} = 166.10$.

The standard deviation of each data point on the trend line was calculated by

$$s^2 = \frac{\sum_{i=1}^n (Y_i - \beta_0 - \beta_1 x_i)^2}{n - 2} = 20.13$$

The standard deviation of β_1 was calculated by

$$s(\beta_1) = \frac{s}{\sqrt{\sum_{i=1}^n (X_i - \bar{X})^2}} = 0.388$$

When the degree of freedom is $n - 2 = 6$ and $p = 0.95$ (a confidence level of 95%), the student distribution t factor [$t_{(0.95, n-2)}$] is 2.447.

Since $|\beta_1| < t_{0.95, n-2} \cdot s(\beta_1) = 0.95$, the slope of this regression function could be neglected.³ Hence, the POD-like of PBNEs CRM was basically stable within one year under 4 °C in darkness.

Section C

Type B standard uncertainty evaluation of characterization

According to law of propagation of uncertainty,⁴ type B relative standard uncertainty of characterization ($u_{B(a_{nano})}$) could be expressed as Eq. C.1:

$$\frac{u_{B(a_{nano})}}{a_{nano}} = \sqrt{\left[\frac{u(V)}{V}\right]^2 + \left[\frac{u(l)}{l}\right]^2 + \left[\frac{u(m_{Fe})}{m_{Fe}}\right]^2 + \left[\frac{u(\Delta A/\Delta t)}{\Delta A/\Delta t}\right]^2 \dots \dots \dots (C.1)}$$

All the potential factors associated with each introduced component were thoroughly analyzed as below without missing or repeating.

C.1 $\frac{u(V)}{V}$

is the relative uncertainty of the total volume of the solution (2400 μL) in the reaction container, derived from two times of 1000 μL and three times of 200 μL

adjustable pipette. According to the data given in Table S2, $\left[\frac{u(V)}{V}\right]^2$ was calculated as

$$\left[\frac{u(V)}{V}\right]^2 = \left[\frac{u(V_{1000\mu\text{L}})}{V_{1000\mu\text{L}}}\right]^2 \times 2 + \left[\frac{u(V_{200\mu\text{L}})}{V_{200\mu\text{L}}}\right]^2 \times 3 = 7.56 \times 10^{-6}$$

C.2 $\frac{u(l)}{l}$

is the relative uncertainty of optical path of cuvette. According to the data given

in Table S2, $\left[\frac{u(l)}{l}\right]^2$ was calculated as

$$\left[\frac{u(l)}{l}\right]^2 = 3.6 \times 10^{-9}$$

$$\text{C.3 } \frac{u(m_{Fe})}{m_{Fe}}$$

is the relative uncertainty of the total Fe element mass contained in added 100 μL PBNEs in the reaction solution, which was calculated by Eq. C.2:

$$\left[\frac{u(m_{Fe})}{m_{Fe}} \right]^2 = \left[\frac{u(V_{Fe})}{V_{Fe}} \right]^2 + \left[\frac{u(C_{Fe})}{C_{Fe}} \right]^2 \dots \dots \dots (\text{C.2})$$

$$C_{Fe} = \frac{C_0(Fe) \times V_0(Fe)}{V_{500 \text{ mL}}}$$

Since

Therefore, Eq. C.2 could be expressed as

$$\left[\frac{u(m_{Fe})}{m_{Fe}} \right]^2 = \left[\frac{u(V_{Fe})}{V_{Fe}} \right]^2 + \left[\frac{u[C_0(Fe)]}{C_0(Fe)} \right]^2 + \left[\frac{u[V_0(Fe)]}{V_0(Fe)} \right]^2 + \left[\frac{u(V_{500 \text{ mL}})}{V_{500 \text{ mL}}} \right]^2$$

with

$$\left[\frac{u(V_{Fe})}{V_{Fe}} \right]^2 = \left[\frac{u(V_{200\mu\text{L}})}{V_{200\mu\text{L}}} \right]^2 = 9 \times 10^{-8}$$

$$\left[\frac{u[V_0(Fe)]}{V_0(Fe)} \right]^2 = \frac{u^2(V_{1000\mu\text{L}}) + u^2(V_{200\mu\text{L}})}{554.8^2} = \frac{0.27^2 + 0.06^2}{554.8^2} = 2.486 \times 10^{-7}$$

$$\left[\frac{u(V_{500 \text{ mL}})}{V_{500 \text{ mL}}} \right]^2 = \left(\frac{0.035}{500} \right)^2 = 4.900 \times 10^{-9}$$

$$\left[\frac{u[C_0(Fe)]}{C_0(Fe)} \right]^2$$

was related to the uncertainties introduced in the measurement of Fe element mass concentration, which should be traced to Fe element standard solution through an unbroken chain of comparisons. The traceability of $C_0(Fe)$ was divided into two parts: (a) the uncertainty introduced when calculating C_0 with the working curve of Eq. A.1; (b) the uncertainty introduced when the Fe element standard solution was diluted to five gradient concentrations of standard solution. The detailed evaluation process was described in Section D. As a result,

$$\left[\frac{u[C_0(Fe)]}{C_0(Fe)} \right]^2 = 5.962 \times 10^{-5}$$

Therefore,

$$\left[\frac{u(m_{Fe})}{m_{Fe}} \right]^2 = 9 \times 10^{-8} + 5.962 \times 10^{-5} + 2.486 \times 10^{-7} + 4.900 \times 10^{-5}$$

C.4 $\frac{u(\Delta A/\Delta t)}{\Delta A/\Delta t}$

is the relative uncertainty of the initial spectral change rate of reaction solution after correcting with reagent blank rate. The uncertainty generated by time was insignificant and could be ignored. The spectrophotometer was issued a calibration certificate by the Metrology Institute, and the expanded uncertainty and coverage factor were given as $U = 0.008$, $k = 2$. Therefore, the standard uncertainty of A is $u(A) = 0.004$.

Since $\Delta A/\Delta t$ was obtained via the linear fitting of the change rate of absorbance with the least square method, it was analysed that the uncertainty of $\Delta A/\Delta t$ consisted of two parts:

(a) Uncertainty introduced by absorbance [$u(\Delta A/\Delta t)$]

The slope of the linear fitting line was

$$b = \frac{n \sum x_i y_i - \sum x_i \sum y_i}{n \sum x_i^2 - (\sum x_i)^2}$$

where b was the slope of the fitting linear; x_i was the measurement time (unit: min); y_i was the absorbance corresponding to each measurement time point.

Substituting $x = 0.1, 0.5, 1.0, 1.5, \text{ and } 2.0$, it was obtained

$$\frac{\Delta A}{\Delta t} = \frac{-4.5A_{0.1} - 2.1A_{0.5} + 0.9A_{1.0} + 3.9A_{1.5} + 6.9A_{2.0}}{11.54}$$

Therefore,

$$u(\Delta A/\Delta t) = \frac{18.3}{11.54} \times u(A) = 0.00634$$

(b) Uncertainty introduced by linear fitting (s_b)

The standard deviation of the slope of liner fitting was

$$s_b = b \sqrt{\frac{1 - r^2}{r^2(n - 2)}}$$

where r was the correlation coefficient of linear fitting and calculated by

$$r = \frac{n \sum x_i y_i - \sum x_i \sum y_i}{\sqrt{|n \sum x_i^2 - (\sum x_i)^2| |n \sum y_i^2 - (\sum y_i)^2|}}$$

It was calculated that s_b was insignificant and could be ignored.

Therefore, the uncertainty of $\Delta A/\Delta t$ was expressed as

$$\left[\frac{u(\Delta A/\Delta t)}{\Delta A/\Delta t} \right]^2 = \left(\frac{0.00634}{\approx 0.27} \right)^2 = 5.523 \times 10^{-4}$$

Section D

The traceability of $C_0(Fe)$

The uncertainty of Fe element mass concentration $[C_0(Fe)]$ of as-prepared PBNEs was traced to Fe element standard solution through an unbroken chain of comparisons, which was divided into two parts:

(a) the uncertainty introduced when calculating C_0 with the working curve of Eq. A.1.

By analyzing the measurement procedure of the Fe element mass concentration

of PBNEs in Section A.2.1, $\frac{u[C_0(Fe)]}{C_0(Fe)}$ could be calculated by Eq. D.1:

$$\left[\frac{u[C_0(Fe)]}{C_0(Fe)} \right]^2 = \left[\frac{u(C_m)}{C_m} \right]^2 + \left[\frac{u(V_{50 mL})}{V_{50 mL}} \right]^2 \times 3 + \left[\frac{u(V_{200 \mu L})}{V_{200 \mu L}} \right]^2 \times 3 + \left[\frac{u(V_{10 \mu L})}{V_{10 \mu L}} \right]^2$$

15.....(D.1)

where $\left[\frac{u(V_{50\text{ mL}})}{V_{50\text{ mL}}} \right]^2 \times 3 + \left[\frac{u(V_{200\ \mu\text{L}})}{V_{200\ \mu\text{L}}} \right]^2 \times 3 + \left[\frac{u(V_{1000\ \mu\text{L}})}{V_{1000\ \mu\text{L}}} \right]^2 \times 15$ was the uncertainty component generated during the process of calcining, dissolving and diluting the as-synthesized PBNEs from 50 μL to 50 mL and was calculated as

$1.431 \times 10^{-6} \cdot \left[\frac{u(C_m)}{C_m} \right]^2$ was the uncertainty introduced when C_m was calculated by Eq. A.1. $u(C_m)$ could be expressed as Eq. D.2:

$$u(C_m) = \frac{s_R}{B_1} \sqrt{\frac{1}{P} + \frac{1}{n} + \frac{(C_m - \bar{C})^2}{\sum_{j=1}^n (C_j - \bar{C})^2}} \dots\dots\dots(D.2)$$

$$s_R = \frac{\sqrt{\sum_{j=1}^n [A_j - (B_0 + B_1 C_j)]^2}}{n - 2} = 2.587 \times 10^{-3}$$

where s_R was the standard deviation of the working curve of absorbance changing with Fe element mass concentrations; $B_1 = 0.004$ was the slope of this working curve; $P = 15$ was the number of measurements of C_m ; $n = 15$ was the number of measurements when determining this working curve. Substituting the data in Table A.1 and Table A.2 into Eq. D.2, it could be obtained :

$$u(C_m) = \frac{2.587 \times 10^{-3}}{4 \times 10^{-3}} \times \sqrt{\frac{1}{15} + \frac{1}{15} + \frac{573.6025}{12000}} = 0.275\ \mu\text{g} \cdot 50\ \text{mL}^{-1}$$

Therefore,

$$\left[\frac{u[C_0(\text{Fe})]}{C_0(\text{Fe})} \right]^2 = \left(\frac{0.275}{36.05} \right)^2 + 1.431 \times 10^{-6} = 5.962 \times 10^{-5}$$

$$u[C_0(\text{Fe})] = 6.959 \times 10^{-3}\ \text{mg} \cdot \text{mL}^{-1}$$

(b) the uncertainty introduced when the Fe element standard solution was diluted to five gradient concentrations of standard solution.

As described in Section A.2.1.1, transferring 20, 40, 60, 80, and 100 μL of Fe element standard solution ($C_s = 1000 \mu\text{g}\cdot\text{mL}^{-1}$) into volumetric flask and diluting to 50 mL, respectively. Take the preparation of 20 $\mu\text{g}\cdot 50 \text{ mL}^{-1}$ Fe element standard solution as an example to calculate the uncertainty introduced by dilution:

Since

$$C_{20\mu\text{L}} = \frac{C_s \times V_{20\mu\text{L}}}{V_{50\text{ml}}}$$

Therefore,

$$\begin{aligned} \frac{u(C_{20\mu\text{L}})}{C_{20\mu\text{L}}} &= \sqrt{\left[\frac{u(C_s)}{C_s}\right]^2 + \left[\frac{u(V_{20\mu\text{L}})}{V_{20\mu\text{L}}}\right]^2 + \left[\frac{u(V_{50\text{ml}})}{V_{50\text{ml}}}\right]^2} = \sqrt{\left(\frac{4.0415}{1000}\right)^2 + \left(\frac{0.0}{20}\right)^2} \\ &= 5.036 \times 10^{-3} \end{aligned}$$

$$u(C_{20\mu\text{L}}) = 5.036 \times 10^{-3} \times 20 \mu\text{g}/50 \text{ mL} = 2.01 \times 10^{-3} \mu\text{g}\cdot\text{mL}^{-1}$$

It was analyzed that this uncertainty was insignificant and could be ignored compared with the uncertainty introduced when calculating C_0 with the working curve.

Therefore, the uncertainty of $[C_0(\text{Fe})]$ of as-synthesized PBNEs was

$$\left[\frac{u[C_0(\text{Fe})]}{C_0(\text{Fe})}\right]^2 = 5.962 \times 10^{-5}$$

References

- 1 J. Gao, X. Ran, C. Shi, H. Cheng, T. Cheng and Y. Su, One-step Solvothermal Synthesis of Highly Water-soluble, Negatively Charged Superparamagnetic Fe₃O₄ Colloidal Nanocrystal Clusters, *Nanoscale*, 2013, **5**, 7026-7033.
- 2 Nanotechnologies — Measurement Method for Peroxidase-like Activity of Iron Oxide Nanoparticles, In *GB/T 37966-2019*, National Technical Committee on Nanotechnology of Standardization Administration, Beijing, China, 2019.

- 3 Reference Materials-Guidance for Characterization and Assessment of Homogeneity and Stability, In *ISO Guide 35:2017*, International Organization for Standardization, Geneva, Switzerland, 2017.
- 4 Uncertainty of Measurement—Part 3: Guide to the Expression of Uncertainty in Measurement (GUM:1995). In *ISO/IEC Guide 98-3*, International Organization for Standardization, Geneva, Switzerland, 2008.